Journal of CO2 Utilization 83 (2024) 102794

Contents lists available at ScienceDirect

Journal of CO2 Utilization

journal homepage: www.elsevier.com/locate/jcou

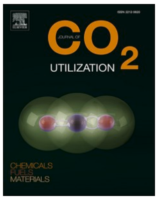

# Microwave thermal pre-treatment and calcination of biomineralised sorbents for calcium looping

María Erans [a,*], Gabriela Durán-Jimenez [b], José M. Rodríguez [b], Lee Stevens [b], Chris Dodds [b]

[a] Department of Chemical Engineering, ETSE, Universitat de València, Av. Universitat s/n, Burjassot, Valencia 46100, Spain
[b] Faculty of Engineering, University of Nottingham, NG7 2RD, United Kingdom

ARTICLE INFO

*Keywords:*
$CO_2$ capture
Eggshell
Calcium looping
Microwave heating
Thermal pretreatment

ABSTRACT

Waste eggshells have been investigated as biomineralised $CO_2$ sorbents for the calcium looping cycle due to their high Ca content, low cost, availability, and high $CO_2$ uptake. This work investigates a novel heat-pre-treatment using eggshells as raw material. The eggshells were simultaneously calcined and thermally pre-treated via microwave heating using different powers and times whilst maintaining the same input energy in a single mode cavity reactor. The calcined eggshells were characterised using standard characterisation techniques such as TGA and isotherms of $N_2$ adsorption at 77 K. The dielectric properties were measured using the cavity perturbation technique at 2.45 GHz. Numerical electromagnetic simulations were performed using COMSOL Multiphysics and results were used to optimise the experimental setup. The treated materials were subjected to carbonation/calcination cycles in order to assess their suitability as a calcium-looping sorbent. The sorbent that exhibited a more stable $CO_2$ uptake was the one treated at the highest power (800 W) 4.5 mmol $CO_2$/g sorbent after 20 cycles under mild calcination conditions. Adsorbents prepared at 400, 600 and 800 W displayed similar $CO_2$ uptake after 20 cycles when the calcination conditions were under more realistic conditions.

## 1. Introduction

The increase of $CO_2$ emissions and, therefore, in $CO_2$ concentration in the atmosphere has increased from 280 ppm in the preindustrial era to an average of 417 ppm in 2022 [1]. Moreover, it has been estimated that the mean global temperature has already increased by approximately 1.5 °C since the Industrial Revolution due to these anthropogenic greenhouse gas emissions [2]. To mitigate the effects of climate change, a portfolio of green energy technologies needs to be urgently deployed for the energy, transportation and industrial sectors.

One of these technologies is carbon capture and storage (CCS), which removes carbon from large point sources using different technologies. Calcium looping is a promising second-generation carbon capture technology. It utilises a Ca-based sorbent that absorbs and desorbs $CO_2$ during carbonation and calcination cycles [3]. The advantages of Ca-based sorbents compared to other high-temperature sorbents are the low price of the raw materials (i.e. limestone and dolomite) due to their wide availability [4]. Also, these materials usually possess high $CO_2$ uptake 0.78 $gCO_2/gCaO$, as well as fast kinetics of $CO_2$ capture and especially regeneration reactions [5–7]. These technologies have attracted vast amounts of research due to the promising results reached at pilot scale [8–10].

Limestone is the most common natural source of calcium carbonate. However, there are natural alternatives that could be used as a Ca-based sorbent, such as eggshells, snail shells, scallop shells and clam shells [11]. Other researchers have also investigated chicken and fish bones as natural calcium carbonate sources [12]. They concluded that these materials were cost-effective, but the authors question if these waste-derived sorbents could be produced in the required quantities. Sacia et al. [13] assessed the suitability of acid treatment for these materials using acetic acid solutions and reported that acid pre-treated samples performed better in Thermogravimetric Analysis TGA. The $CO_2$ uptake of these materials has been compared to that of limestone [14], where it was reported that the uptake of eggshells and mussel shells was similar to that of limestone over 50 cycles.

Eggshells are comprised mainly of calcium carbonate (94 % weight) [15], which makes it a promising candidate as a biomineralised Ca-based sorbent. Annual worldwide production of eggs was around 80 million tons in 2019 [16]. Most waste-derived eggshells are accumulated on-site without any pre-treatment [17]. Therefore, most discarded eggshells could be used as a $CO_2$ sorbent in calcium looping. Other waste sources have also been proposed as promising raw materials for calcium looping, such as scallop shells, mussel shells and Mactra Veneriformis

---

* Corresponding author.
*E-mail address:* maria.erans@uv.es (M. Erans).

https://doi.org/10.1016/j.jcou.2024.102794
Received 20 February 2024; Received in revised form 24 April 2024; Accepted 26 April 2024
Available online 3 May 2024

**Nomenclature**

| | |
|---|---|
| $\lambda_0$ | free space wavelength |
| $\lambda_c$ | cut of wavelength |
| $c$ | speed of light |
| $f_0$ | operation frequency |
| $a$ | length of the broad side of the waveguide |
| $\omega$ | is the angular frequency |
| $\mu_0$ | is the permeability of free space |
| $\mu_r$ | relative permeability |
| $\varepsilon_0$ | permittivity of free space |
| $\varepsilon_r$ | relative permittivity |
| $\sigma$ | conductivity. |
| BET | Brunauer–Emmett–Teller model |
| CCS | Carbon Capture and Storage |
| FEM | Finite Element Method |
| PUI | Power Uniformity Index |
| TGA | Thermogravimetric analyser |
| VNA | vector network analyser |
| XRD | X Ray Diffraction |

(MV) shells, with results that demonstrated the superior performance of MV during a series of cycles [18]. Other studies have investigated the use of cockle shells, which showed promising results with 0.60–0.65 g $CO_2$/g sorbent [19], sorbent and high surface area and pore volume [20].

One of the main challenges of the calcium looping technology is the reactivity decay of the Ca-based sorbent over a long number of carbonation/calcination cycles, which is mainly caused by sintering. To overcome this challenge, different options have been proposed. Namely, doping, pelletisation, thermal pre-treatment, and the production of synthetic sorbents have all been widely investigated [21,22]. Thermal activation has been widely used as a pre-treatment as it minimises the reactivity decay over a long series of cycles [23–25] due to the formation of a hard skeleton that stabilises the CaO crystal in subsequent carbonation/calcination cycles. Thermal pre-treatment and reactivation have clear benefits; they are simple and inexpensive. Nevertheless, energy is still needed to carry out this treatment [21]. This will result in more energy demand and possibly more $CO_2$ being produced, decreasing the overall amount of $CO_2$ avoided.

Microwave heating has been proposed as a potentially sustainable source of heating for a broad range of applications as it can offer several advantages such as volumetric heating, selective heating, shorter processing times, low thermal inertia, rapid on/off operability and control, and increased product yields and quality. In particular, volumetric heating can overcome heat transfer limitations for relatively low thermal conductivity products, in particular at high temperatures where conventional heating becomes inefficient, by delivering heat directly within the material volume instead of delivering to its surface by convection or radiation, which then relies on thermal conduction to raise internal temperatures [26–30]. Moreover, it uses electric energy directly without the need for fossil fuels [31,32], with the potential to be operated with clean energy sources; however, to the authors' knowledge, there are no studies assessing the suitability of microwave heating to calcine/pre-treat any calcium looping sorbent. However, high-temperature microwave processes pose some serious challenges that require addressing to allow for industrialisation, such as poor treatment homogeneity, reactor lack of robustness, construction materials, and compatible material transport technologies [33,34].

In this work, eggshell, which is a waste and low-cost source of calcium carbonate, has been investigated as a $CO_2$ sorbent. Moreover, a novel calcination/thermal pre-treatment was carried out via electromagnetic heating of eggshells to produce highly stable Ca-based sorbents for calcium looping. The dielectric properties of the raw eggshell were measured to understand their interaction with microwaves and used for the optimisation of the experimental setup by electromagnetic simulation. Moreover, an in-depth characterisation of the pre-treated and untreated biomineralised sorbents was performed. In addition, the cyclic $CO_2$ capacity was investigated during 20 carbonation/calcination cycles, both in mild and realistic calcination conditions, to assess if the reactivity decay can be minimised via microwave thermal pre-treatment, similar to conventional heating.

## 2. Materials and methods

### 2.1. Materials

The eggshells were recovered from domestic use in Nottinghamshire (UK). They were washed with deionised water and dried for 24 h at 105 °C. Then, they were washed with an acetic acid solution (15 % vol.) to separate the shell from the organic membrane and to chemically pre-treat the sample [35]. After the separation, the eggshells were washed with deionised water and dried at 105 °C for 24 h. The dried material was pulverised until a fine powder was created (<100 μm).

### 2.2. Thermal and dielectric characterisation of eggshells

X-ray diffraction was performed on the raw material with a Bruker D8 Advance DAVINCI ranging from 10 to 70° 2θ. TGA analysis was performed on the raw eggshells in pure Nitrogen ($N_{2)}$ at 1 bar, 100 ml/min, where the sample was heated at 5 ºC/min until 900 ºC.

The dielectric properties of the treated eggshells were attained near 2.45 GHz, which is a frequency globally allocated as an Industrial, Scientific and Medical (ISM) frequency band, suitable for industrial heating applications. The method used was the cavity perturbation technique using an HP 8753 vector network analyser (VNA), which allow for precise measurement of relatively low-loss materials at high temperatures [36,37]. Approximately 10 mg of the sample at a packed density of 1.3 g/cm$^3$ was positioned in a 3 mm ID quartz tube supported on Triton Kaowool (ceramic fibre). The sample was heated to the desired temperature inside a tube furnace and kept at temperature for 5 min. It was then moved to the cavity for measurement using a motorised stage. The dielectric properties were calculated using the difference in cavity response (i.e., resonant frequency and quality factor) between the loaded and an empty tube holder. The experiments were done in triplicate.

### 2.3. Microwave calcination of eggshells

The microwave experiments were carried out in the system shown in Fig. 1. It comprises a 2 kW, 2.45 GHz generator (Sairem), and an automatic three-stub tuner (S-TEAM STHD v1.5). The automatic tuner was used for impedance matching to minimise the power reflected by the system and to measure the absorbed energy into the sample. The tuner is connected to a rectangular $TE_{10}$ single-mode cavity with a sliding short. The reactor consisted of a quartz tube (34 mm ID) with a sintered disc acting as a distributor plate where 20 g of the powdered eggshell was placed through a choke tube that prevents microwave leakage, sized according to [38]. $N_2$ was used as an inert atmosphere during the experiments.

Before the calcination experiments, the optimal sliding short position was determined to locate the sample in a high electric field zone, allowing for effective power coupling and ensuring optimal treatment homogeneity. The short position was first estimated using transmission line theory, which can be sufficient in cases where the sample is relatively small compared to the applicator. However, in this work, given the sample size, further optimisation was carried out considering the sample and holder properties using COMSOL Multiphysics RF module COMSOL Multiphysics RF module based on the finite element method

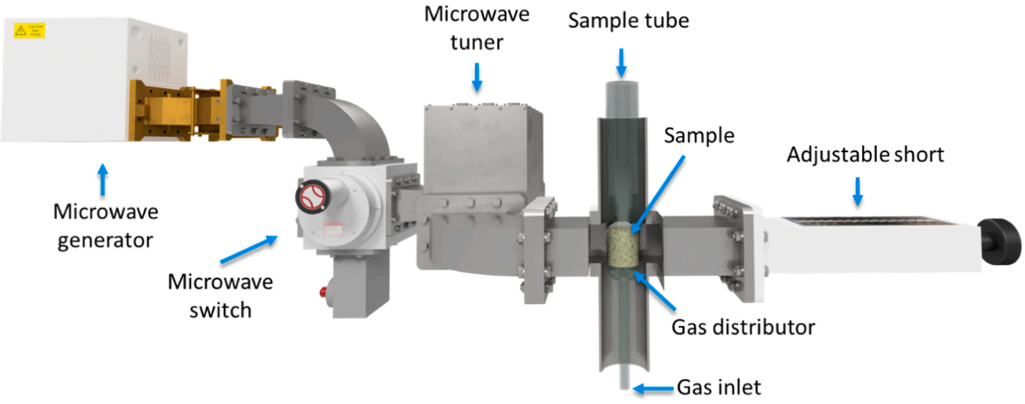

**Fig. 1.** Schematic of the microwave calcination setup.

(FEM) [39].

Upon terminating the waveguide in a short circuit, the electric field becomes zero at the termination for the dominant mode $TE_{10}$, as the field is polarised in parallel to the metal surface. The wave is reflected with the opposite phase of the incoming wave and superimposes with it, creating a standing wave pattern with an initial zero electric field at the short, and electric fields peaks at distances equal to odd multiples of a quarter of the guided wavelength from the short, following:

$$d_{E-\max,n} = \quad (n+1)\lambda_g/4 \tag{1}$$

Where n = 0, 1, 2, 3,…, and $\lambda_g$is the guided wavelength given by

$$\lambda_g = \lambda_0 \Bigg/ \sqrt{1-\left(\frac{\lambda_0}{\lambda_c}\right)^2} \tag{2}$$

Where $\lambda_0$ is the free-space wavelength, and $\lambda_c$ is the cut-off wavelength which can be determined as

$$\lambda_0 = \frac{c}{f_0} \tag{3}$$

$$\lambda_c = 2a \tag{4}$$

Where c is the speed of light 299,792,458 m/s, $f_0$ is the operation frequency, and $a$ is the length of the broad side of the waveguide being used, in this case, 86.36 mm, resulting in $\lambda_0 = 122.5$ mm, $\lambda_c = 172.7$ mm and $\lambda_g = 173.8$ mm. This results in values of $d_{E-\max} = 43.5, 86.9, 130.3, \ldots$mm. Given the applicator's total length of 150 mm, the sample position at its centre, and the sliding short minimum length of 40 mm, the minimum practical length would be 115 mm, so a position of $d_{E-\max}$ of 130.3 mm was selected, resulting in a short starting position of 55.3 mm.

The system was modelled in COMSOL, with geometry discretised with a maximum element size of λ/5, with a finer λ/10 element size within the material, where λ represents the wavelength inside of the material (i.e. $\lambda = \lambda_0/\sqrt{\varepsilon_r'}$, with $\lambda_0$ being the free-space wavelength). The dielectric material properties used were the ones measured in this work and modelled as isotropic media. The wave equations for the electric fields ($E$) are solved in the frequency domain, following Eq. 5 [39]

$$\nabla \times \frac{1}{\mu_r}(\nabla \times E) - \omega^2 \varepsilon_0 \mu 0 \left(\varepsilon_r - \frac{j\sigma}{\omega \varepsilon_0}\right) E = 0 \tag{5}$$

where $\omega$ is the angular frequency, $\mu_0$ is the permeability of free space, $\mu_r$ is the relative permeability,$\varepsilon_0$ is the permittivity of free space, $\varepsilon_r$ is the relative permittivity, σ is the conductivity.

A parametric sweep of the short position is performed for various sets of material properties within the expected variation to determine the position that can provide superior overall uniformity of treatment. The uniformity is assessed using the power uniformity index (PUI), which measures the uniformity of power dissipation within a volume, zero being an entirely uniform distribution of power dissipation [38,40].

Exploratory tests were undertaken to assess the input energy necessary for the total calcination of the samples (less than 10 % carbonate in the resulting material). After the exploratory tests, different power levels and times were established to investigate the effect of these parameters on the same amount of input energy. The studied cases were: (i) 400 W for 30 min, (ii) 600 W for 20 min and (iii) 800 W for 15 min. For comparison purposes, conventional calcination experiments were performed in a muffle furnace where the material was kept at 850 °C for 2 h in an air atmosphere. These experiments aim to investigate how power density might affect $CO_2$ uptake. The samples were denoted as XX-YYY-ZZZ, where XX denotes the heating mechanism used (MW microwave, C conventional), YYY denotes the temperature (°C) for conventional heating and power (W) for microwave-treated samples, and ZZZ denote treatment time in minutes. The selected experiments are shown in Table 1.

### 2.4. *Characterisation of treated eggshells*

The textural properties of the samples were calculated from the adsorption/desorption isotherms of $N_2$ at−196 °C using a Micromeritics®ASAP2420 apparatus from 0.00005 to 0.99 relative pressure ($P/P_0$). The specific surface area was calculated using the Brunauer–Emmett–Teller (BET) model [41] between 0.05 and 0.20 ($P/P_0$). The total pore volume was calculated using the BJH model with Harkins-Jura correction.

### 2.5. *Cyclic $CO_2$ capture*

The capture capacity of the sorbents was evaluated via TGA using a Q500 TA instrument. The carbonation was performed under 15% vol $CO_2$ (1 bar 100 ml/min) at 650 ºC for 15 min. On the other hand, calcination was performed either for 5 min at 950 ºC in pure $CO_2$ for realistic industrial calcination conditions or for 5 min at 850 ºC in pure $N_2$ (1 bar 100 ml/min) to assess the effect of mild calcination conditions. 20 cycles were performed for each material at each condition in order to investigate the reactivity decay of the microwave-treated sorbents.

**Table 1**
Experimental matrix.

| Sample | Calcination | Temperature (ºC) | Power (W) | Time (min) |
|---|---|---|---|---|
| **C-850–120** | Conventional | 850 | n/a | 120 |
| **MW-400–30** | Microwave | n/a | 400 | 30 |
| **MW-600–20** | Microwave | n/a | 600 | 20 |
| **MW-800–15** | Microwave | n/a | 800 | 15 |

## 3. Results and discussion

### 3.1. Characterisation of eggshells

The results from the XRD of eggshells can be found in Fig. 2. The eggshells are highly crystalline, as expected, with only calcium carbonate peaks present, while the calcined eggshell present only calcium oxide peaks [42]. The decomposition curve of eggshells is widely known with the decomposition of organic material present in the membrane is decomposed from 200 ºC to 400 ºC and from 600 ºC calcination starts to occur at a very rapid rate typically found in Ca-based materials [43].

### 3.2. Dielectric properties

The dielectric properties are presented in Fig. 3, where dielectric constant (a), and dielectric loss (b)are shown. Up to 200 °C, the behaviour is dominated by moisture, exhibiting a relatively low loss factor as samples have been dried [44,45]. Between 200 and 400 °C, a slow increase in dielectric properties related to membrane decomposition can be observed. After 400 °C, a sharp rise of the dielectric constant and loss factor appears as the weakening of bonds and thermal expansion allows for stronger ionic polarisation. This behaviour suggests that for an eventual process scale-up, preheating the feed material above 500 °C could be desirable to ensure it is sufficiently microwave absorbent for an efficient treatment.

The results from the textural characterisation can be found in Table 2. The highest BET surface area and total pore volume is present in MW-400–30 (9 $m^2/g$ and 0.074 $cm^3/g$), where the calcination was carried out in a slower manner, and its porosity was preserved. On the contrary, MW-800–15 has the lowest pore volume and surface area, 3.9 $m^2/g$ and 0.016 $cm^3/g$, respectively, and is where the higher microwave power density was delivered in the sample due to the higher power intensity. The data suggests that the increase in the power intensity led to an instantaneous temperature increase causing the sintering of the CaO grains and, therefore, reducing total pore volume and surface area. This is consistent with previous findings in literature where thermally pre-treated samples were found to have lower pore volume before treatment [46]. The difference in total pore volume between MW400–30 and C-850–120 might be due to carbonation temperatures in the MW-treated sample as the power supplied to the sample was low; therefore, lower temperatures should have been reached. This lower temperature achieved with lower microwave power levels resulted in minimised sintering during the calcination-thermal pre-treatment simultaneous step.

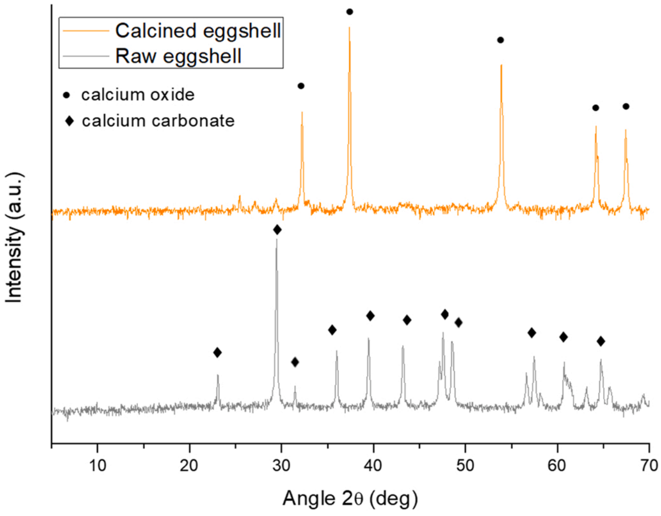

**Fig. 2.** X RD pattern of raw and calcined eggshells.

The $N_2$ adsorption-desoprtion isotherms at −196 °C are depicted in Fig. 4. The adsorption by sample calcined with MW-400–30 is the highest, implying the highest pore volume and specific surface area. This agrees with those of the samples' specific surface area and total pore volume, as presented in Table 2. According to the IUPAC classification, the adsorption isotherms correspond to a Type II, which is representative of nonporous materials or macroporous structures or open voids [47]. It should be noted that the sample MW-400–30 possesses larger surface area in comparison with the other samples. This suggests the modest microwave treatment modifies the structural properties of the sample, allowing the increase in the surface area and pore volume. Microwave calcination also modifies the chemical properties of the eggshell, creating more active sites for $CO_2$ uptake. The hysteresis loop observed at higher pressures is associated to the capillary condensation in mesopores. It can be noted that isotherms do not reach plateau at $>0.95\ P/P_0$, suggesting that larger macropores exist beyond 180 nm.

The isotherms presented in Fig. 4 are typical type II and combined with type IV, as reported in the literature for calcium-based materials [48]. The particle size distribution shown in Fig. 5 confirms that the samples are mainly formed by macropores. After calcination using different conditions, the sample MW-400–30 displayed a reduction in pore size. This reduction can be associated with the creation of smaller pores due to the release of $CO_2$ from the calcium carbonate. The larger pore size for samples MW-600–20, MW-800–15 and C-850–120 can be as result of higher calcination temperatures that lead to the elimination of internal walls in the skeleton of structure, generating macropores and the growth of calcium oxide grain sizes due to sintering at high temperature. This finding is of great relevance the sorbent's pore structure significantly affects the reaction and diffusion of $CO_2$.

### 3.3. Microwave treatment uniformity

The starting short position obtained by transmission line theory calculations of 55.3 mm, was checked preliminary using COMSOL Multiphysics, without sample. The electric field distribution is shown in Fig. 6, showcasing the standing wave pattern with a maximum electric field at the centre of the applicator as predicted, where the sample will be positioned.

Given this work's relatively large sample size, further optimisation was required. The sample and its holder tube are incorporated into the model. The sample properties were considered as isothermal and evaluated for 200, 400, 600 and 800 °C, based on the values shown in Fig. 3. The sample holder made of quartz is modelled considering a permittivity of $4 - j0.0001$ [49]. The PUI for different sliding short lengths and the set of sample properties for different temperatures are shown in Fig. 7. Two operational zones of high uniformity for the full range of properties can be identified around the minimum PUI values on the chart. As the minimum sliding short length is 40 mm, the top range was selected for operation, with a sliding short position of 123 mm.

To illustrate the significant difference in treatment uniformity, two extreme cases are showcased in Fig. 8, where the electric field distribution is shown for sample properties at 600 °C. In the first case, a sliding short length of 102.5 mm was selected, with a PUI of 0.8, representing a low uniformity case. In this case, the fields are primarily concentrated in the left side of the sample, closer to the generator. In the second case, a short length of 123 mm was used, with a PUI of 0.3, representing a close to optimal uniformity, where the electric fields appear to be more uniformly distributed within the sample, with the maximum at its centre. This analysis highlights the importance of determination of sliding short length in this type of experimental system, as a poor selection can result in uneven heating and localised overheating.

### 3.4. Cyclic $CO_2$ capture capacity

It has been reported that carbonation conversion occurs in two

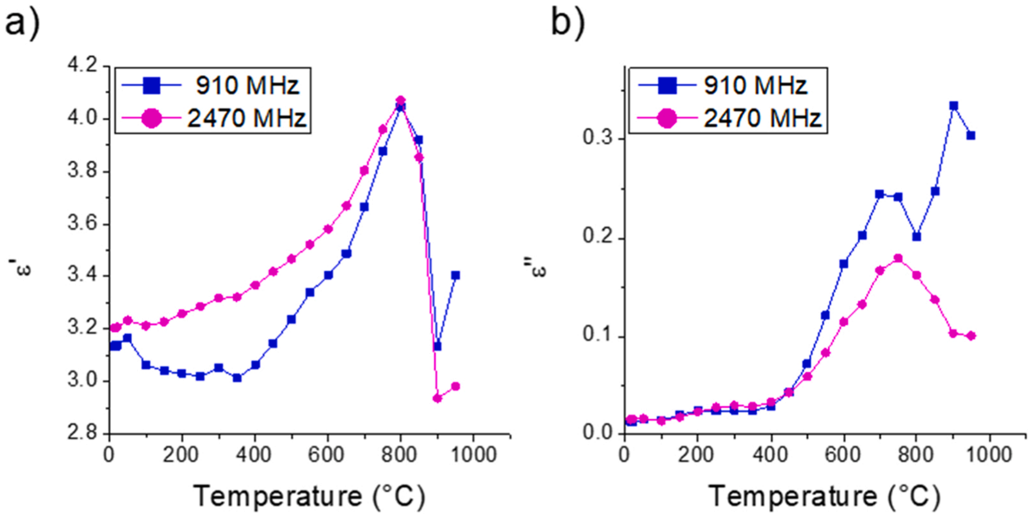

**Fig. 3.** Dielectric properties of eggshells: a) dielectric constant, b) dielectric loss.

**Table 2**
Specific surface area of conventional and microwave-treated samples.

| Sample | Surface area ($m^2/g$) | Total pore volume ($cm^3/g$) |
|---|---|---|
| **C-850–120** | 6.7 | 0.016 |
| **MW-400–30** | 9.0 | 0.074 |
| **MW-600–20** | 4.0 | 0.019 |
| **MW-800–15** | 3.9 | 0.016 |

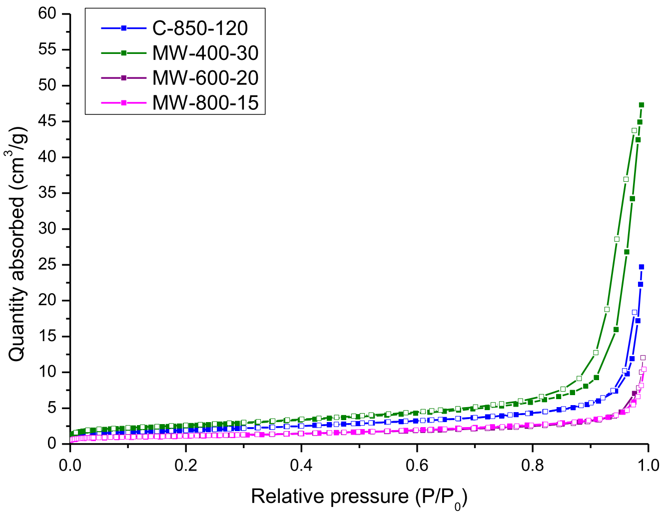

**Fig. 4.** $N_2$ adsorption-desorption isotherms of eggshell-derived sorbents (solid points: adsorption process, hollow points: desorption process).

stages; the first is influenced by the surface area, while the second stage is controlled by diffusion [48]. The first stage usually happens fast and is controlled by chemical kinetics, while the second occurs slowly and is controlled by diffusion. Results shown in Fig. 9, which were performed in mild calcination conditions (850 °C in pure $N_2$), suggest the sample MW-800–15 has a better gas-solid reaction than MW-400–30 at the $CO_2$ concentration studied (15 % vol). This could be a result of MW-400–30 having narrower pores, reducing the conversion by particles of lower size diameter. In this regard, the differences in the $CO_2$ uptake shown by the samples are more significant during the diffusion-controlled stage. Sample MW-400–30 with narrow pores has higher resistance to diffusion than the other samples, resulting in a reduction in $CO_2$ mass transfer and, therefore, uptake.

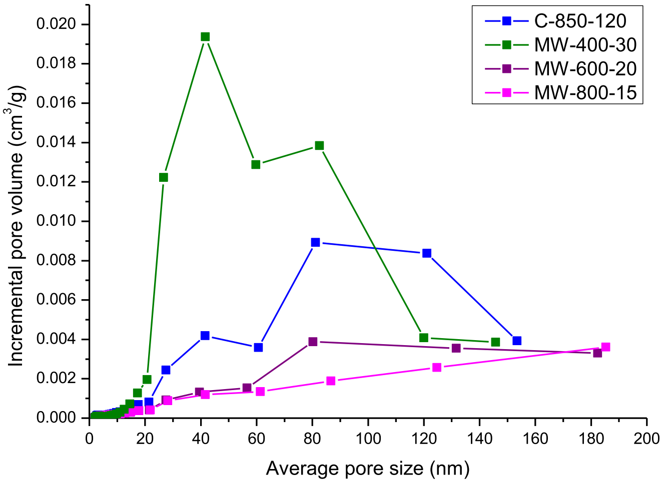

**Fig. 5.** Pore size distribution of conventional and microwave-treated samples using BJH (with Harkins-Jura correction) method.

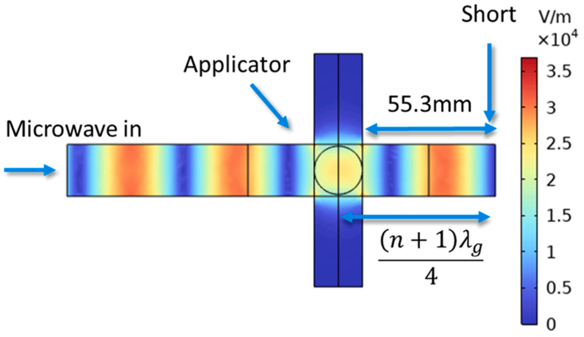

**Fig. 6.** Electric field distribution without sample at short position of 55.3 mm, determined using transmission line theory. Centre-cut side-view.

Fig. 10 shows the comparison between the conversion of all the studied sorbents during 20 cycles under these mild calcination conditions. It has been previously reported that during cycling, sorbent particles undergo two simultaneous types of mass transfer: bulk diffusion, linked to the formation and decomposition of $CaCO_3$, and ion diffusion within the crystal structure of CaO. The ion diffusion in CaO plays a role

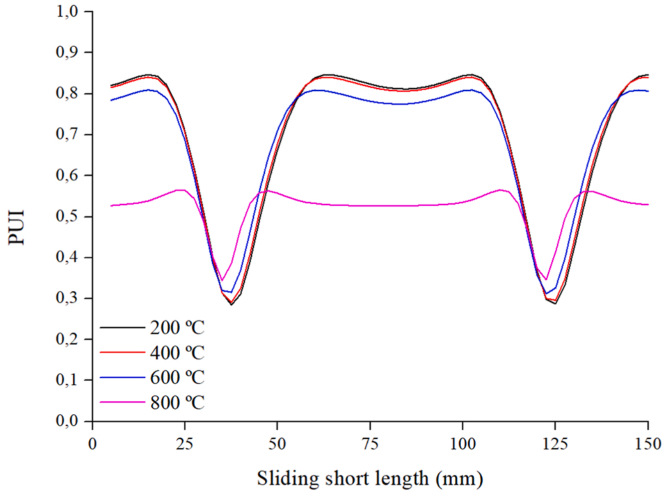

**Fig. 7.** PUI for different sliding short lengths and sample properties for 200, 400, 600 and 800 °C.

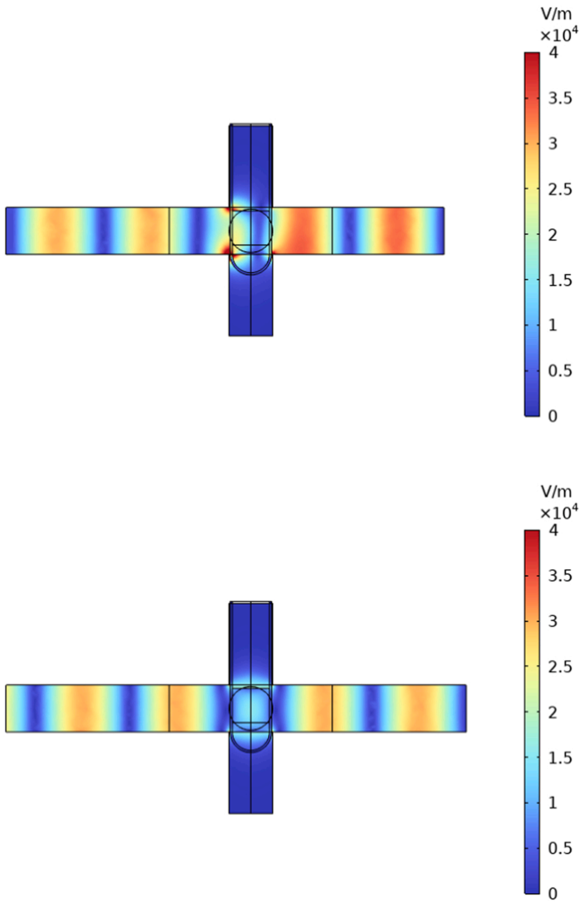

**Fig. 8.** Electric field distribution for sliding short of length (a) 102.5 and (b) 123 mm. for sample properties at 600 °C.

in stabilising its crystal structure, though it does not impact particle morphology or the corresponding carbonation conversions [50]. Bulk mass transfer is predominant during the formation and decomposition of $CaCO_3$, causing significant changes in morphology, such as sintering and the loss of small pores, consequently affecting sorbent activity. Throughout $CO_2$ cycles, competition arises between ion diffusion and bulk mass transfer, forming two distinct structures or skeletons. One is an internal unreacted structure, functioning as a robust skeleton stabilising and protecting particle morphology, including its pore structure. Simultaneously, an external structure forms where carbonation/calcination processes take place. This phenomenon was initially explained by Lysikov et al. [50]; in this work, a two-skeleton model was proposed where these skeletons, in this context, do not pertain to the particles themselves but rather to the pores [51]. The designation "external" indicates that this portion of the skeleton is exposed to the pores and enveloped by the gas filling those pores. Here, it can be observed in the first cycle similar conversion values are obtained for MW-800–15 and C-850–120 in the with 42.6 and 40.2 %, respectively. However, after 20 cycles the thermally pretreated/calcined sample that achieved the highest possible temperature (MW-800–15) during the decomposition reaction showed a conversion of 26.4 vs a 20.9 % conversion of the conventionally calcined limestone, which is a 5.5 % increase in residual conversion. This finding is consistent with literature as it has been found that thermal pretreatment with high temperature increases carbonation conversion in a long series of cycles [51]. Previous studies have also explored the influence of time and temperature on the $CO_2$ uptake of thermally pre-treated samples. This work further reduced the time needed for the calcination/pre-treatment as these studies found that short pre-treatment periods are effective (6 h at different temperatures) [51]. It is key to note that the effectiveness of the thermal pretreatment when subsequent calcinations are performed in $N_2$ is related to the chemical composition of the sorbent [52]. It is expected that sorbents with low impurities (i.e., high purity limestone) show negligible benefits from pretreatment. However, eggshells present a wide variety of impurities making this the ideal treatment [43]. It is worth noting that eggshells typically have lower conversion than limestone, with literature values of around 5 % after 20 cycles [53].

In Fig. 11, the $CO_2$ uptake is shown in 20 carbonation/calcination cycles for all the synthesised sorbents. In this series of experiments, the calcination was performed under realistic conditions (in a pure $CO_2$ atmosphere). It could be expected that the microwave treatment produced similar results to those of Fig. 10. However, when the calcination reaction was performed under a $CO_2$ atmosphere the sorbents behaved in a different manner. With these conditions, the sample that retained a high $CO_2$ uptake was conventionally calcined with a residual 2.36 mmol/g after 20 cycles. However, the sorbents synthesised with microwave energy, MW-800–15, MW-600–20 and MW-400–30 showed lower $CO_2$ uptakes with 2.24, 2.23 mmol/g and 1.94 mmol/g, respectively.

Interestingly, when the conditions of the calcination reaction are realistic (in a pure $CO_2$ atmosphere) the materials behave in a similar manner regardless of the calcination and thermal pre-treatment from the first cycle. This could mean that the sintering is identical for all materials irrespective of the development of the two-skeleton model. It is known that $CO_2$ partial pressure during the calcination reaction also plays a crucial role in the sintering phenomenon [54–56]. Therefore, the potential benefit of the thermal pre-treatment seen previously under mild calcination conditions is cancelled by realistic reaction conditions in a long cycle series. Thus, this extra reaction step would have negligible benefits compared to the cost in terms of reactivity behaviour. Another factor that needs to be addressed is the possibility of decarbonising the calcination process via microwave energy. This would mean using renewable energy to power the microwave generator instead of burning fossil fuels (i.e., natural gas) as a heat source for the endothermic calcination reaction. This has added benefits as it leads towards the electrification of technologies, which could be valuable in future years. If electrification was the end goal, it can be observed that similar $CO_2$ uptakes can be obtained with shorter reaction times, 15 min versus 120 min in conventional heating. Suppose this calcination option was to be considered at a larger scale, a more in-depth study should be performed to optimise $CO_2$ uptake in short reaction times, which would be feasible using microwave energy. In Fig. 12, conversions of all materials are shown for 20 cycles under these realistic calcination conditions. All

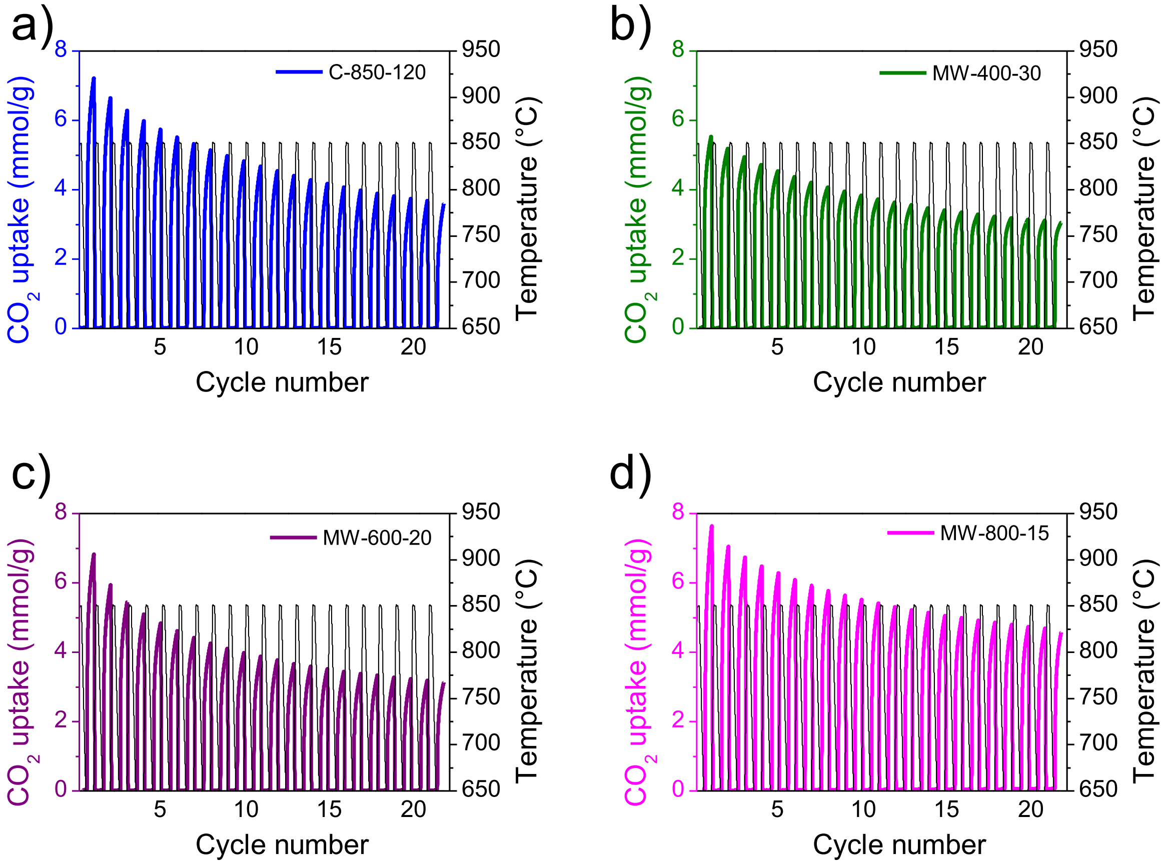

**Fig. 9.** $CO_2$ uptake of a) C-850–120, b) MW-400–30, c) MW-600–20 and d) MW-800–15, carbonation 15 min at 650 °C in 15 % vol $CO_2$ and calcination at 850 °C in pure $N_2$.

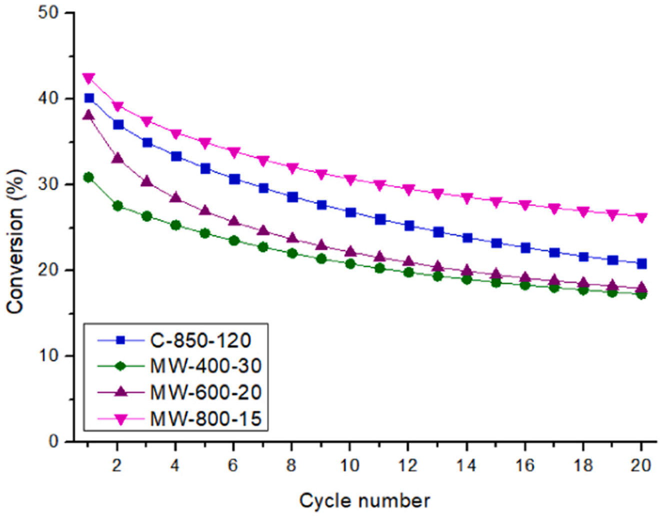

**Fig. 10.** Cyclic conversions of all samples: carbonation 15 min at 650 °C in 15 % vol $CO_2$ and calcination at 850 °C in pure $N_2$.

materials reached a similar conversion, with the highest being C-850–120 with 13.2 % and MW-400–30, MW-600–20 and MW-800–15 with 10.8, 12.5 and 12.5 % respectively.

It should be noted that these TGA experiments have limitations as their conditions are different from scaled-up $CO_2$ capture systems where fluidised beds are used. In these systems phenomena such as attrition and fragmentation of the sorbent are present. These phenomena modify the residence time of the particles in the reactors, which typically decreases the degree of $CO_2$ capture.

## 4. Conclusions

The results demonstrated that eggshells is promising waste-derived material for calcium looping that maintains a relatively high $CO_2$ uptake and could be potentially used in large-scale calcium looping systems as a sole sorbent or in combination with limestone. Different microwave powers and reaction times were used to maintain a consistent energy input. The sample MW-800–15 exhibited maximum carbonation after 20 cycles, despite having minimal pore volume and surface area. This could be due to the formation of a hard skeleton that stabilises the structure of the pores, preventing further sintering in subsequent cycles. Nevertheless, the microwave treatment's limited applicability under realistic conditions, coupled with the high capital cost of installing a microwave system and the added system complexity for power/industrial plants decarbonising, raises concerns about its practical feasibility. It is worth noting that while short calcination reaction times are achievable with this microwave heating, further studies into the techno-economics of the process are required to assess its scale-up feasibility and commercial prospects.

## CRediT authorship contribution statement

**Maria Erans:** Writing – review & editing, Writing – original draft, Methodology, Investigation, Formal analysis, Data curation, Conceptualization. **Gabriela Durán-Jimenez:** Writing – review & editing, Methodology, Investigation, Formal analysis, Data curation. **José Miguel Rodríguez:** Writing – review & editing, Methodology, Investigation, Formal analysis, Data curation. **Lee Stevens:** Writing – review & editing, Resources, Formal analysis, Data curation. **Chris Dodds:**

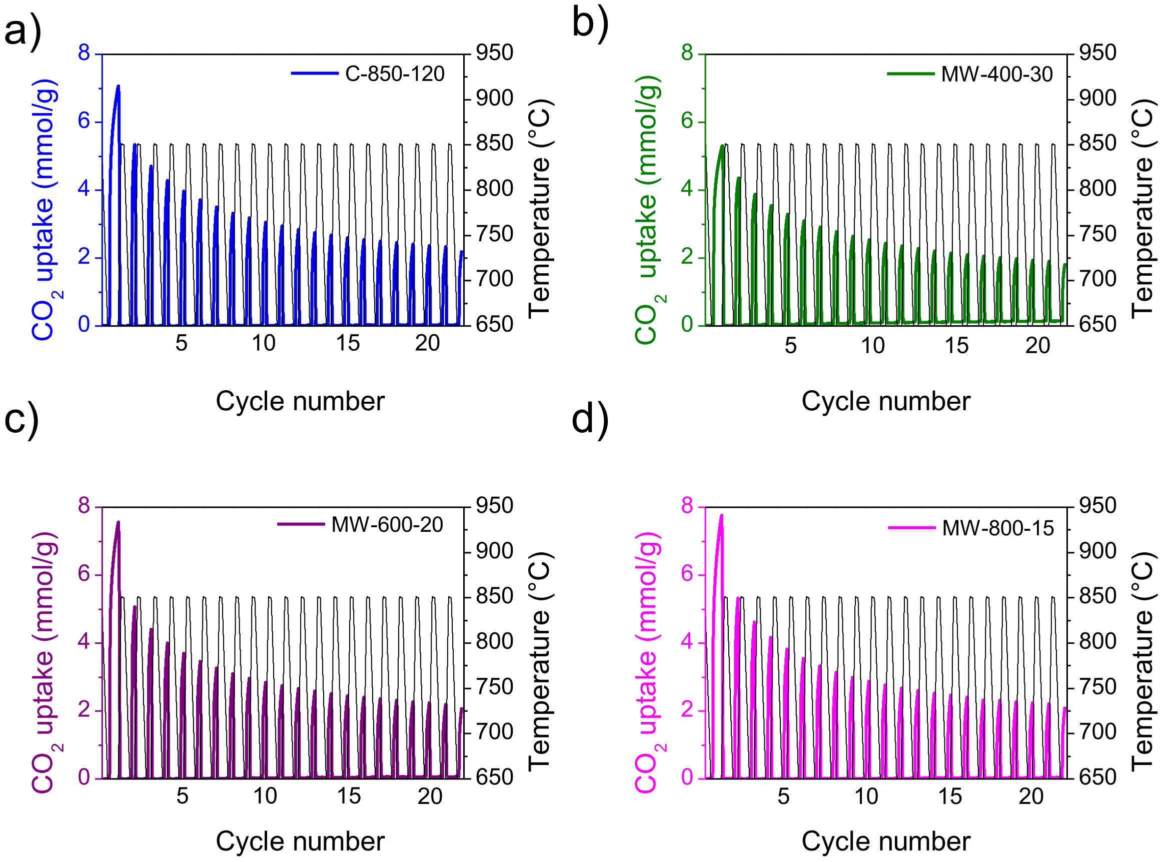

Fig. 11. $CO_2$ uptake of a) C-850–120, b) MW-400–30, c) MW-600–20 and d) MW-800–15, carbonation 15 min at 650 °C in 15 % vol $CO_2$ and calcination at 850 °C in pure $CO_2$.

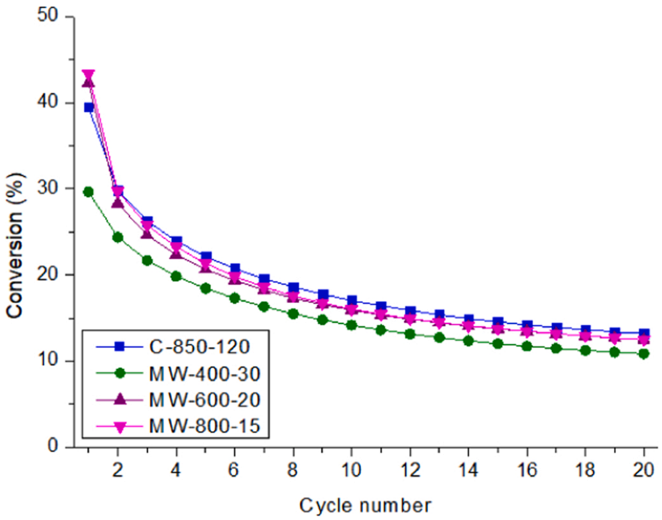

Fig. 12. Cyclic conversions of all samples: carbonation 15 min at 650 °C in 15 % vol $CO_2$ and calcination at 850 °C in pure $CO_2$.

Writing – review & editing, Resources.

## Declaration of Competing Interest

The authors declare that they have no known competing financial interests or personal relationships that could have appeared to influence the work reported in this paper.

## Data availability

Data will be made available on request.

## Acknowledgements

M.E. is grateful for Grant RYC2021–031428-I funded by MCIN/AEI/10.13039/501100011033 and by European Union NextGenerationEU/PRTR. Authors would like to acknowledge funding from MCIN/AEI/European Union NextGenerationEU/PRTR through project TED2021–129555B-I00.

## References

[1] E. Dlugokencky, P. TansGlobal trends in atmospheric carbon dioxide, NOAA/GML Gml.Noaa.Gov/Ccgg/Trends/ (Accessed September 16, 2023) (2023).
[2] The Intergovernmental Panel on Climate Change, Global warming of 1.5 °C, 2020.
[3] T. Shimizu, T. Hirama, H. Hosoda, K. Kitano, M. Inagaki, K. Tejima, A twin fluid-bed reactor for removal of $CO_2$ from combustion processes, Chem. Eng. Res. Des. 77 (1999) 62–68.
[4] H.C. Mantripragada, E.S. Rubin, Calcium looping cycle for $CO_2$ capture: performance, cost and feasibility analysis, Energy Procedia 63 (2014) 2199–2206.
[5] J. Wang, L. Huang, R. Yang, Z. Zhang, J. Wu, Y. Gao, Q. Wang, D. O'Hare, Z. Zhong, Recent advances in solid sorbents for $CO_2$ capture and new development trends, Energy Environ. Sci. 7 (2014) 3478–3518.
[6] A.M. Kierzkowska, R. Pacciani, C.R. Müller, CaO-based $CO_2$ sorbents: from fundamentals to the development of new, highly effective materials, ChemSusChem 6 (2013) 1130–1148.
[7] S. Choi, J.H. Drese, C.W. Jones, Adsorbent materials for carbon dioxide capture from large anthropogenic point sources, ChemSusChem: Chem. Sustain. Energy Mater. 2 (2009) 796–854.
[8] B. Arias, M.E. Diego, J.C. Abanades, M. Lorenzo, L. Diaz, D. Martínez, J. Alvarez, A. Sánchez-Biezma, Demonstration of steady state $CO_2$ capture in a 1.7 MWth calcium looping pilot, Int. J. Greenh. Gas. Control 18 (2013) 237–245.
[9] J. Ströhle, M. Junk, J. Kremer, A. Galloy, B. Epple, Carbonate looping experiments in a 1 MWth pilot plant and model validation, Fuel 127 (2014) 13–22.

[10] M.-H. Chang, W.-C. Chen, C.-M. Huang, W.-H. Liu, Y.-C. Chou, W.-C. Chang, W. Chen, J.-Y. Cheng, K.-E. Huang, H.-W. Hsu, Design and experimental testing of a 1.9 MWth calcium looping pilot plant, Energy Procedia 63 (2014) 2100–2108.

[11] S. Castilho, A. Kiennemann, M.F.C. Pereira, A.P.S. Dias, Sorbents for $CO_2$ capture from biogenesis calcium wastes, Chem. Eng. J. 226 (2013) 146–153.

[12] N. Deshpande, B. Yuh, Screening of multiple waste animal shells as a source of calcium sorbent for high temperature $CO_2$ capture, Sustain. Eng. Res 23 (2013) 227–232.

[13] E.R. Sacia, S. Ramkumar, N. Phalak, L.-S. Fan, Synthesis and regeneration of sustainable CaO sorbents from chicken eggshells for enhanced carbon dioxide capture, ACS Sustain Chem. Eng. 1 (2013) 903–909.

[14] M. Ives, R.C. Mundy, P.S. Fennell, J.F. Davidson, J.S. Dennis, A.N. Hayhurst, Comparison of different natural sorbents for removing $CO_2$ from combustion gases, as studied in a bench-scale fluidized bed, Energy Fuels 22 (2008) 3852–3857.

[15] M.B. Kannan, K. Ronan, Conversion of biowastes to biomaterial: an innovative waste management approach, Waste Manag. 67 (2017) 67–72.

[16] Accessed 17/11/2023, Poultry trend 2019, n.d.

[17] H. Faridi, A. Arabhosseini, Application of eggshell wastes as valuable and utilizable products: a review, Res. Agric. Eng. 64 (2018) 104–114.

[18] Y. Li, C. Zhao, H. Chen, L. Duan, X. Chen, $CO_2$ capture behavior of shell during calcination/carbonation cycles, Chem. Eng. Technol.: Ind. Chem. -Plant Equip. -Process Eng. -Biotechnol. 32 (2009) 1176–1182.

[19] M. Mohamed, N.A. Rashidi, S. Yusup, L.K. Teong, U. Rashid, R.M. Ali, Effects of experimental variables on conversion of cockle shell to calcium oxide using thermal gravimetric analysis, J. Clean. Prod. 37 (2012) 394–397.

[20] N.A. Rashidi, M. Mohamed, S. Yusup, A study of calcination and carbonation of cockle shell, (2011).

[21] M. Erans, V. Manovic, E.J. Anthony, Calcium looping sorbents for $CO_2$ capture, Appl. Energy 180 (2016) 722–742.

[22] J. Chen, L. Duan, Z. Sun, Review on the development of sorbents for calcium looping, Energy Fuels 34 (2020) 7806–7836.

[23] V. Manovic, E.J. Anthony, G. Grasa, J.C. Abanades, CO2 looping cycle performance of a high-purity limestone after thermal activation/doping, Energy Fuels 22 (2008) 3258–3264.

[24] V. Manovic, E.J. Anthony, Thermal activation of CaO-based sorbent and self-reactivation during $CO_2$ capture looping cycles, Environ. Sci. Technol. 42 (2008) 4170–4174.

[25] H. Chen, C. Zhao, Development of a CaO-based sorbent with improved cyclic stability for $CO_2$ capture in pressurized carbonation, Chem. Eng. J. 171 (2011) 197–205.

[26] S. Das, A.K. Mukhopadhyay, S. Datta, D. Basu, Prospects of microwave processing: an overview, Bull. Mater. Sci. 32 (2009) 1–13, https://doi.org/10.1007/s12034-009-0001-4.

[27] S. Nomanbhay, M.Y. Ong, A review of microwave-assisted reactions for biodiesel production, Bioengineering 4 (2017) 57, https://doi.org/10.3390/bioengineering4020057.

[28] F. Motasemi, M.T. Afzal, A review on the microwave-assisted pyrolysis technique, Renew. Sustain. Energy Rev. 28 (2013) 317–330, https://doi.org/10.1016/j.rser.2013.08.008.

[29] C. Yin, Microwave-assisted pyrolysis of biomass for liquid biofuels production, Bioresour. Technol. 120 (2012) 273–284, https://doi.org/10.1016/j.biortech.2012.06.016.

[30] K.E. Haque, Microwave energy for mineral treatment processes — a brief review, Int. J. Min. Process 57 (1999) 1–24, https://doi.org/10.1016/S0301-7516(99)00009-5.

[31] P.P. Falciglia, P. Roccaro, L. Bonanno, G. De Guidi, F.G.A. Vagliasindi, S. Romano, A review on the microwave heating as a sustainable technique for environmental remediation/detoxification applications, Renew. Sustain. Energy Rev. 95 (2018) 147–170.

[32] T.J. Appleton, R.I. Colder, S.W. Kingman, I.S. Lowndes, A.G. Read, Microwave technology for energy-efficient processing of waste, Appl. Energy 81 (2005) 85–113.

[33] D. Beneroso, T. Monti, E.T. Kostas, J. Robinson, Microwave pyrolysis of biomass for bio-oil production: scalable processing concepts, Chem. Eng. J. 316 (2017) 481–498, https://doi.org/10.1016/j.cej.2017.01.130.

[34] E. Binner, E. Lester, S. Kingman, C. Dodds, J. Robinson, A review of microwave coal processing, J. Microw. Power Electromagn. Energy 48 (2014) 35–60.

[35] M. Imani, M. Tahmasebpoor, P.E. Sánchez-Jiménez, J.M. Valverde, V. Moreno, Improvement in cyclic $CO_2$ capture performance and fluidization behavior of eggshell-derived $CaCO_3$ particles modified with acetic acid used in calcium looping process, J. $CO_2$ Util. 65 (2022) 102207.

[36] S. Altarawneh, M. Al-Harahsheh, A. Buttress, C. Dodds, J. Rodriguez, S. Kingman, Microwave selective heating of electric arc furnace dust constituents toward sustainable recycling: contribution of electric and magnetic fields, J. Ind. Eng. Chem. 104 (2021), https://doi.org/10.1016/j.jiec.2021.09.001.

[37] A. Parkash, J.K. Vaid, A. Mansingh, Measurement of dielectric parameters at microwave frequencies by cavity-perturbation technique, IEEE Trans. Micro Theory Tech. 27 (1979) 791–795, https://doi.org/10.1109/TMTT.1979.1129731.

[38] J. Rodriguez, J. Ampuero, W. Valderrama, A. Buttress, C. Dodds, S. Kingman, H. Carrasco, S-band elliptical–cylindrical cavity resonator for material processing, Micro Opt. Technol. Lett. 64 (2022), https://doi.org/10.1002/mop.33431.

[39] COMSOL Multiphysics(r) v. 6.2., The RF Module User's Guide, Stockholm, Sweden, 2023. ⟨www.comsol.com/blogs⟩.

[40] G. Tiwari, S. Wang, J. Tang, S.L. Birla, Analysis of radio frequency (RF) power distribution in dry food materials, J. Food Eng. 104 (2011) 548–556, https://doi.org/10.1016/j.jfoodeng.2011.01.015.

[41] M. Thommes, K. Kaneko, A.V. Neimark, J.P. Olivier, F. Rodriguez-Reinoso, J. Rouquerol, K.S.W. Sing, Physisorption of gases, with special reference to the evaluation of surface area and pore size distribution (IUPAC Technical Report), Pure Appl. Chem. 87 (2015) 1051–1069.

[42] N. Um, Enhancement of arsenic removal efficiency from mining waste water by accelerated carbonation, 2014. ⟨https://www.researchgate.net/publication/288376751⟩.

[43] A. Nawar, M. Ali, A.H. Khoja, A. Waqas, M. Anwar, M. Mahmood, Enhanced $CO_2$ capture using organic acid structure modified waste eggshell derived CaO sorbent, J. Environ. Chem. Eng. 9 (2021) 104871, https://doi.org/10.1016/j.jece.2020.104871.

[44] S.E. Etuk, U.W. Robert, J.B. Emah, O.E. Agbasi, Dielectric properties of eggshell membrane of some select bird species, Arab J. Sci. Eng. 46 (2021) 769–777.

[45] P. Krongkitsiri, W. Krongkitsiri, S. Phukird, U. Tipparach, A comparison of dielectric properties of eggshells from free-range system and control-range system, Mater. Today Proc. 47 (2021) 3617–3623.

[46] K.O. Albrecht, K.S. Wagenbach, J.A. Satrio, B.H. Shanks, T.D. Wheelock, Development of a CaO-based $CO_2$ sorbent with improved cyclic stability, Ind. Eng. Chem. Res. 47 (2008) 7841–7848, https://doi.org/10.1021/ie8007743.

[47] W.T. Tsai, J.M. Yang, C.W. Lai, Y.H. Cheng, C.C. Lin, C.W. Yeh, Characterization and adsorption properties of eggshells and eggshell membrane, Bioresour. Technol. 97 (2006) 488–493.

[48] S.A. Salaudeen, S.H. Tasnim, M. Heidari, B. Acharya, A. Dutta, Eggshell as a potential $CO_2$ sorbent in the calcium looping gasification of biomass, Waste Manag. 80 (2018) 274–284.

[49] A.J. Buttress, J.M. Rodriguez, A. Ure, R.S. Ferrari, C. Dodds, S.W. Kingman, Production of high purity silica by microfluidic-inclusion fracture using microwave pre-treatment, Min. Eng. 131 (2019) 407–419, https://doi.org/10.1016/j.mineng.2018.11.025.

[50] A.I. Lysikov, A.N. Salanov, A.G. Okunev, Change of $CO_2$ carrying capacity of CaO in isothermal recarbonation−decomposition cycles, Ind. Eng. Chem. Res. 46 (2007) 4633–4638, https://doi.org/10.1021/ie0702328.

[51] V. Manovic, E.J. Anthony, Thermal activation of CaO-based sorbent and self-reactivation during $CO_2$ capture looping cycles, Environ. Sci. Technol. 42 (2008) 4170–4174, https://doi.org/10.1021/es800152s.

[52] V. Manovic, E.J. Anthony, G. Grasa, J.C. Abanades, $CO_2$ looping cycle performance of a high-purity limestone after thermal activation/doping, Energy Fuels 22 (2008) 3258–3264, https://doi.org/10.1021/ef800316h.

[53] J. Arcenegui-Troya, P.E. Sánchez-Jiménez, A. Perejón, J.M. Valverde, R. Chacartegui, L.A. Pérez-Maqueda, Calcium-looping performance of biomineralized $CaCO_3$ for $CO_2$ capture and thermochemical energy storage, Ind. Eng. Chem. Res. 59 (2020) 12924–12933, https://doi.org/10.1021/acs.iecr.9b05997.

[54] F. García-Labiano, A. Abad, L.F. de Diego, P. Gayán, J. Adánez, Calcination of calcium-based sorbents at pressure in a broad range of $CO_2$ concentrations, Chem. Eng. Sci. 57 (2002) 2381–2393, https://doi.org/10.1016/S0009-2509(02)00137-9.

[55] J.M. Valverde, P.E. Sanchez-Jimenez, L.A. Perez-Maqueda, Calcium-looping for post-combustion $CO_2$ capture. On the adverse effect of sorbent regeneration under $CO_2$, Appl. Energy 126 (2014) 161–171, https://doi.org/10.1016/j.apenergy.2014.03.081.

[56] V. Manovic, J.-P. Charland, J. Blamey, P.S. Fennell, D.Y. Lu, E.J. Anthony, Influence of calcination conditions on carrying capacity of CaO-based sorbent in $CO_2$ looping cycles, Fuel 88 (2009) 1893–1900, https://doi.org/10.1016/j.fuel.2009.04.012.